The Pumping SeaSoar: A High-Resolution Seawater Sampling Platform

BURKE HALES

College of Oceanic and Atmospheric Sciences, Oregon State University, Corvallis, Oregon

TARO TAKAHASHI

Lamont-Doherty Earth Observatory, Columbia University, Palisades, New York

(Manuscript received 16 February 2001, in final form 18 January 2002)

ABSTRACT

The first results obtained with the Lamont Pumping SeaSoar (LPS), a combination measurement and sampling platform towed by a research ship at speeds of 6–7 kt, are presented. The system allows not only measurement of a suite of oceanographic parameters with in situ sensors, but also delivery of seawater samples through a 750-m tube (5/16-in. inner diameter) to a shipboard laboratory for chemical analyses, while undulating from near the surface to depths near 200 m. Here the performance of the system is demonstrated, and the time lag and signal smearing associated with the seawater sampling scheme are qualitively analyzed. The time lag was determined by comparing salinity determined from measurements of temperature, conductivity, and pressure made in situ by the sensors mounted on the towed body, with salinity determined from temperature and conductivity measurements made in the shipboard outlet of the sample stream. It varied smoothly from 10.8 to 11.5 min over 24 h of sampling, independent of the depth of the fish. The time lag was determined with precision of better than 5 s, corresponding to vertical precision of about 1 m. Smearing of signals due to mixing in the tube was approximated by a Gaussian filter with a time constant of 7.5–10 s, corresponding to a vertical scale of about 2 m.

1. Introduction

With the onset of satellite observation of properties like sea surface temperature (SST) and ocean color measures of chlorophyll abundance, the importance of short horizontal length scale (10–100 km) features to the overall ocean character is increasingly recognized. The use of towed undulating vehicles, beginning in the early 1970s, has led to great advances in high-speed, high-spatial-resolution oceanographic survey work (Aiken et al. 1977; Aiken 1981, 1985; Dessureault 1975; Hermann and Dauphinee 1980; Strass 1992). The most widely used of these systems is the SeaSoar (Pollard 1986; Griffiths and Pollard 1992; Bahr and Fucile 1995), currently marketed by Chelsea Instruments, Ltd. SeaSoar has been used for a number of mesoscale studies of ocean features, such as fronts, eddies, and coastal jets (e.g., Read and Pollard 1992; Pollard et al. 1995; Rudnick 1996; Rudnick and Luyten 1996; Barth et al. 1998; Huyer et al. 1998; Shearman et al. 1999; Barth and Bogucki 2000; Barth et al. 2000, and many others). SeaSoars have been deployed carrying sensors for a variety of in situ measurements, including temperature, salinity, photosynthetically active radiation (PAR), chlorophyll fluorescence, dissolved oxygen, beam attenuation, bioluminescence, and video plankton recording. With the exception of electrodes for the measurement of dissolved oxygen, however, no chemical measurements of adequate quality have been included in these surveys. In separate work, Friedrich and others developed a system for pumping seawater from depth back to a shipboard lab for chemical analyses (Friederich and Codispoti 1987; Codispoti et al. 1991). This system allowed collection of large-volume water samples pumped up from precise depths, but was intended only for vertical profiling at a fixed location. Measurement of lateral variability was never attempted, however, and the analyses were never optimized for the faster dive and ascent rates experienced with towed undulating vehicles.

Our goal was to bring basic chemical oceanography up to speed with the physical and bio-optical measurements in the mesoscale. To that end we mounted a high-pressure positive-displacement pump on a SeaSoar towed by a cable with a sample delivery tube embedded in its core, thus marrying the pumped sampling system of Friederich and Codispoti with this towed undulating vehicle. The SeaSoar carried an array of sensors for in

Corresponding author address: Dr. Burke Hales, College of Oceanic and Atmospheric Sciences, Oregon State University, 104 Ocean Admin. Bldg., Corvallis, OR 97331-5503.
E-mail: bhales@oce.orst.edu

situ measurement of depth, temperature, salinity, PAR, chlorophyll-*a* fluorescence, and dissolved oxygen concentrations. At the shipboard end of the sample tube, we determined salinity; nitrate, phosphate, silicate, and total carbon dioxide concentrations; and carbon dioxide partial pressure. These shipboard measurements, excluding the temperature/conductivity-based salinity measurement, all involve significant improvements in sampling frequency relative to standard approaches and will be discussed in future publications.

During the development of the Lamont Pumping SeaSoar (LPS) system, the following technical problems critical to its performance were addressed: 1) potential lack of control of the system due to excessive hydrodynamic drag caused by the large tow cable diameter, which was necessary for incorporation of the water sampling tube; 2) difficulty of pumping water from depths in excess of 200 m in the water column to the ship; 3) inability to accurately correct for the lag associated with sample transit through the sampling tube, and therefore ignorance of the depth and location where the sample was taken; and 4) axial mixing in the sample tube that might so severely degrade the signals present in the water column that reconstruction of in situ spatial distributions of chemical parameters would be impossible. In the following sections we address solutions to each of these problems specifically, and describe the performance of the system during the first deployments in the Ross Sea, Antarctica.

2. Methods

a. System construction

The pumping SeaSoar consists broadly of four components: 1) the SeaSoar vehicle; 2) the sampling pump; 3) the tow cable, with the sample tube contained within its core and fairing designed to minimize drag; and 4) the specialized winch to contain the faired tow cable.

The SeaSoar itself is largely unchanged since its first commercial production by Chelsea Instruments, Ltd. (East Molesey, Surrey, United Kingdom; www.chelsea.co.uk). Briefly, it is a towed body (hereafter referred to as the ''fish'') designed to be pulled by a ship at speeds of up to 10 kt, while undulating between the surface and depths of a few hundred meters. The fish contains a hydraulically driven ram, which rotates the ''wings,'' or diving vanes, which in turn control the fish's position and dive/climb rates. The hydraulic system is powered by an impeller on the aft end of the fish, which turns as water flows past due to the ship's motion. Space inside the body is adequate for carrying CTD units and associated sensors, and other oceanographic equipment. We included a fairly standard package of sensors—two temperature–conductivity (T–C) pairs (SeaBird Electronics, Inc., Bellevue, Washington; www.seabird.com), mounted low and forward outside the fish body; a fluorometer for chlorophyll measurement (WetStar; Wetlabs Inc., Philomath, Oregon; www.wetlabs.com); an electrode for dissolved oxygen measurement (Beckmann DO; provided by SeaBird); and an irradiance sensor for PAR measurement (Biospherical QSP200-L; www.biospherical.com; also provided by SeaBird); and a custom wing-angle sensor (J. Ardai, Lamont-Doherty Earth Observatory, Palisades, New York)—all interfaced with a SeaBird 9+ CTD unit containing a Digiquartz pressure sensor.

We used the remaining space inside the body to mount our sampling pump. The pump consisted of a positive-displacement, plunger-style pump head (Teel, model 5P247) driven by a submersible well-pump motor (Franklin Electric, model 2345294). The pump is capable of delivering a constant flow of 2 gal min^{-1} at pressures from 0–1000 psi. The 1.5-hp motor runs on three-phase 480-V ac power (drawing roughly 2 A), supplied from the ship through the tow cable. Because the pressure this pump is capable of generating exceeds the tube's working pressure and that under which it will burst, we put a pressure relief valve at the outlet of the pump set to relieve at 300–400 psi. Any flow that led to tube pressures in excess of this was bled out in situ and not forced up the tube.

The 750-m tow cable was a custom construction (Cortland Cable Inc., Cortland, New York). It consisted of a Kevlar strength member, braided over twenty-four 24-awg copper conductors, in turn wrapped around a 5/16-in. inner diameter (i.d.) by 7/16-in. outer diameter (o.d.) nylon-11 tube (300-psi rated pressure, 1000-psi burst pressure; Universal Plastics, Inc., Mentor, Ohio). The cable was wrapped overall by a braided nylon jacket, and had an o.d. of 0.72 in. Twelve of the conductors were combined into three sets of four to carry the three phases of the pump power; the remaining conductors were used to deliver power to and collect data from the CTD unit, and to control the hydraulic wing-positioning system. The cable was terminated by attaching a diamond-wrap load-bearing termination to the cable a few feet from the end; this was in turn secured to the tow bridle on the fish. The tube and conductors were then brought into the interior of the fish body where they were connected to the pump and CTD unit, respectively.

Because this cable is roughly twice the diameter of standard SeaSoar tow cables, hydrodynamic drag during towing will also be doubled. As a result, fairing is probably essential to minimize this drag and maintain some control over the towed body. We used the Flexnose plastic fairing (Series 894; now manufactured by Indal, Inc., Toronto, Ontario, Canada), which has a tear-drop-shaped cross section, 1 in. wide and 4 in. long. Flexnose-faired cable cannot be wrapped upon itself on a winch drum; it must be wrapped in a single layer. Cable of this length and diameter requires a very large winch drum to be wrapped in a single layer. We used a custom winch with a 6-ft-diameter by 10.5-ft-long drum (SeaMac Marine Products, Houston, Texas). Because of the size of this winch and the difficulty of shipping it,

we had it permanently mounted in a standard 20-ft shipping container with removable doors built into one side. For operation, the whole container was lifted aboard the ship and bolted to the deck. The doors were removed and the cable paid out directly from the van.

b. System control

We were unsatisfied with the control system provided by Chelsea Instruments. During a brief test cruise off the West Coast of the United States in August of 1996, we undulated the fish between 5 and 220 m with dive and climb rates up to 60 m min^{-1} but felt that we had inadequate control over dive and climb rates. Since we expected slower dive/climb rates to be necessary for adequate depth resolution with slower top-side analytical systems, a new control system was required. Our control routine, written in LabView software (National Instruments, Austin, Texas; www.ni.com), was designed to deliver constant dive and climb rates between maximum and minimum depths, thus generating an up–down sawtooth undulation pattern. We achieved this through a two-level feedback scheme where we controlled wing position in response to the difference between target and actual dive and climb rates. The in situ wing-angle sensor allowed us to control wing angle directly, using the difference between target and measured position, with the Chelsea hydraulic wing driver. The SeaBird pressure sensor allowed us to compare the actual dive rate of the LPS to the target dive rate. When the target dive rate was greater than the actual dive rate, we increased the wing angle incrementally until the rates matched; when the target dive rate was less than the actual, we decreased the wing angle. The reverse procedure was followed during ascent.

c. Transfer function quantification

Comparison of the data collected at the shipboard outlet of the water sample stream with that collected using sensors aboard the fish requires the shipboard data to be adjusted for the effects of the transfer through the tube to the ship. This transfer function was assessed by comparing time series of salinity calculated from in situ measurements of temperature (T), conductivity (C), and pressure to that calculated from T–C measurements at the shipboard outlet of the water sample stream. The simplest transfer function includes three factors that must be considered: the time lag due to transit through the tube; the offset between the two sensor pairs due to their inherent inaccuracy; and the ''smearing'' of information due to mixing along the tube axis during transit. It is, in principle, possible to find optimum combinations of all three of these; however, there were very few features in the records we collected that showed any unequivocal impact from smearing. We therefore found optimal combinations of lags and salinity offsets as a function of time that corresponded to the minimum deviation between the in situ salinity and the shipboard salinity adjusted for the lag and offset [deviations minimized by Powell's method; Press et al. (1989)]. We then compared the adjusted shipboard record with the in situ record to find sharp features that had been smeared in transit through the tube. Once such features were identified, we simulated the smearing in the tube by filtering the in situ signal with Gaussian filters with various time constants until the filtered in situ signal resembled the shipboard signal.

3. Results

We successfully deployed the pumping SeaSoar four times during the Southern Ocean Joint Global Ocean Flux Study (JGOFS) Ross Sea Process IV cruise aboard the Research Vessel/Ice Breaker (RVIB) *Nathaniel B. Palmer* during November and December of 1997. Each deployment lasted 24–30 h. Three of the deployments were west–east transects of the JGOFS Ross Sea sampling line, about 300 km long, along 76.5°S between 170°E and 180°. The fourth was a square wave pattern with five parallel 60-km north–south sections about 13 km apart between 76.25° and 76.75°S and 172° and 174°E. Ship speed during these surveys was 6–7 kt. With 500 m of cable paid out (the remainder was left spooled on the winch drum), we undulated the fish between target minimum and maximum depths of 10 and 200 m at selected dive and climb rates of 10–20 m min^{-1}. One up–down cycle took about 25 min to complete. We measured sample flow rates at the shipboard end of the sample stream of about 4 L min^{-1}, independent of the depth of the sample intake.

The tow track from the first of these surveys is shown in Fig. 1. This shows the track of the SeaSoar during 25–26 November 1997, in the early stages of the development of the phytoplankton bloom in the Ross Sea polynya. The sawtooth nature of the track shows the effectiveness with which we were able to control the dive and climb rates at constant values. We selected low dive and climb rates, 10–20 m min^{-1}, as opposed to the $\geq$60 m min^{-1} rates achieved in the earlier test cruise, because we were limited by the speed of our shipboard chemical analytical systems. Analysis times ranged from 2 seconds per analysis (30 min^{-1}) for CO_2 partial pressure to 30 seconds per analysis (2 min^{-1}) for total carbon dioxide, and in order to keep sufficiently high vertical resolution for these measurements we needed to correspondingly decrease the dive and climb rates. For the depth ranges covered and the ship speeds employed, these dive/climb rates gave horizontal resolution of about 2 km at middepths, and twice that at maximum and minimum depths. Minimum depth was intentionally set deep to avoid sea ice; we could have targeted shallower minima in ice-free conditions. Maximum turnaround depth, while an integral part of the control algorithm, was set mostly to coincide with the maximum achievable depths.

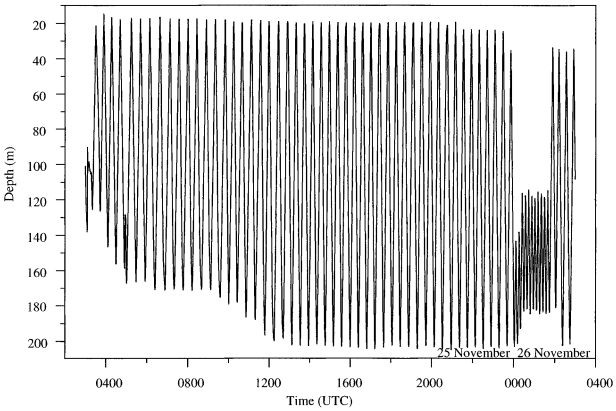

FIG. 1. Pumping SeaSoar depth as a function of time during a 24-h deployment on 25–26 Nov 1997. Target dive and climb rates were 10 db min^{-1} in the early (<0.5 day) part of the record, and then were increased to 15 db min^{-1}. Target minimum depth was 15 db, set deep to avoid surface ice. Target maximum depth was set shallow initially and later increased to achieve the maximum attainable with the LPS (about 200 m, with 500 m of faired cable out at a ship speed of 7 kt). The latter part of the record (26 Nov) shows a period when surface ice cover was especially heavy and we kept the fish deep until we could recover it in open water.

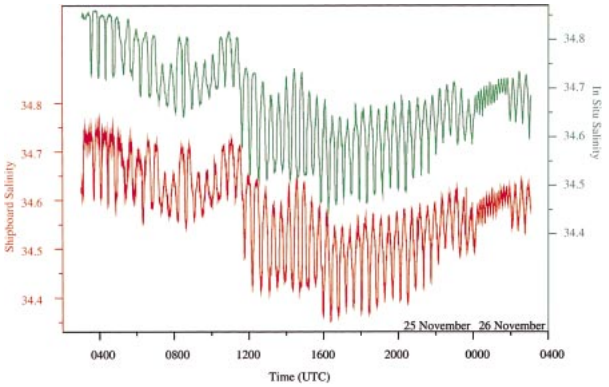

FIG. 2. Time series of salinity as determined from in situ temperature, conductivity, and pressure sensors (green line) and shipboard (red line) temperature and conductivity sensors. The dominant periodicity in the series is from the undulation of the LPS, as shown in Fig. 1. The shipboard salinity lags the in situ salinity by a little less than half of one up–down period because of the transit time of water through the sampling tube from the in situ intake at the fish to the shipboard T–C pair located at the opposite end of the sample tube. Data shown are medians of 1-s bins of 12-Hz (in situ) and 6-Hz (shipboard) measurements, resulting in 1-Hz resolution here.

While salinity measured at the shipboard outlet of the sample stream is not a parameter we expect to use for scientific interpretation, it is the best measure of the transfer function applied to the sample stream by flow through the sample tube. Salinity is conservative, unlike temperature; the sensors have very fast response times, allowing for unequivocal interpretation of the smearing of signals; and we have high-resolution records of the salinity at all times during the deployment; finally, the external mounting of the in situ T–C sensors eliminated salinity–pressure lags that might complicate the comparison of the in situ and shipboard records. Time series of salinity calculated from the in situ T–C and pressure and shipboard T–C measurements during this survey are shown in Fig. 2. From casual inspection of these traces, it is clear that the shipboard trace is a lagged version of the in situ trace, demonstrating the first-order result that water can be pumped from the fish back to the ship with reasonable sample integrity.

We quantified the lag by taking 5-min subsets of the in situ trace (each containing 300 measurements) and finding optimum combinations of the phase lag and sensor offset that produced the minimum deviation between the shipboard trace and the in situ trace. The results of this exercise are shown in Fig. 3. Figure 3a shows the time lag calculated for each subset as a function of time. At the beginning of the deployment, the lag is about 10.5 min, and by the end it has increased to about 11.5 min. This increase is likely due in part to a leak in the pump–tube connection in the fish that developed during the survey, and to slow changes in the bypass pressure of the relief valve. These lag times are consistent with the estimated volume of the pump, tubing, filters, and sensors in the flow path between the fish and the shipboard T–C pair (about 40 L) and the measured flow rates at the shipboard end of the sample stream (about 4 L min^{-1}). The offset between salinity calculated from in situ and shipboard sensors is shown in Fig. 3b. Early in the deployment, salinity calculated from the shipboard T–C pair is 0.02–0.025 higher than the in situ salinity; it is also substantially noisier. After cleaning the shipboard pair by flushing it with a dilute HCl solution the offset between the two reduced to about 0.005, and the noise levels in the shipboard sensor pair substantially diminished. Mean absolute deviations between the lag-adjusted, offset-corrected records are typically about 0.0015.

One method of assessing the errors introduced by pumping is to compare the lag-adjusted, offset-corrected shipboard salinity trace with the in situ trace. We did this by interpolating the lag and offset corrections shown in Figs. 3a and 3b, respectively, and applying these to the shipboard data. Demonstrating the agreement is somewhat difficult since the corrected shipboard trace is nearly indistinguishable from the in situ trace when the two full records are plotted together. In Fig. 4a we plot the two salinity estimates against each other, and this plot shows tight 1:1 correlation and an average deviation of 0.0015 salinity units for the entire dataset. In Fig. 4b we show a 5-min subsample of the in situ and adjusted shipboard salinity, demonstrating the sensitivity to the lag correction. The mean absolute deviation between the in situ and adjusted shipboard salinity in this subsample is 0.0016 for the optimum lag (10 min, 44 s); the average deviation is less than 10^{-4}, demonstrating that most of the deviation between the two records is due to sensor noise and not consistent offset. Adjusting the lag by

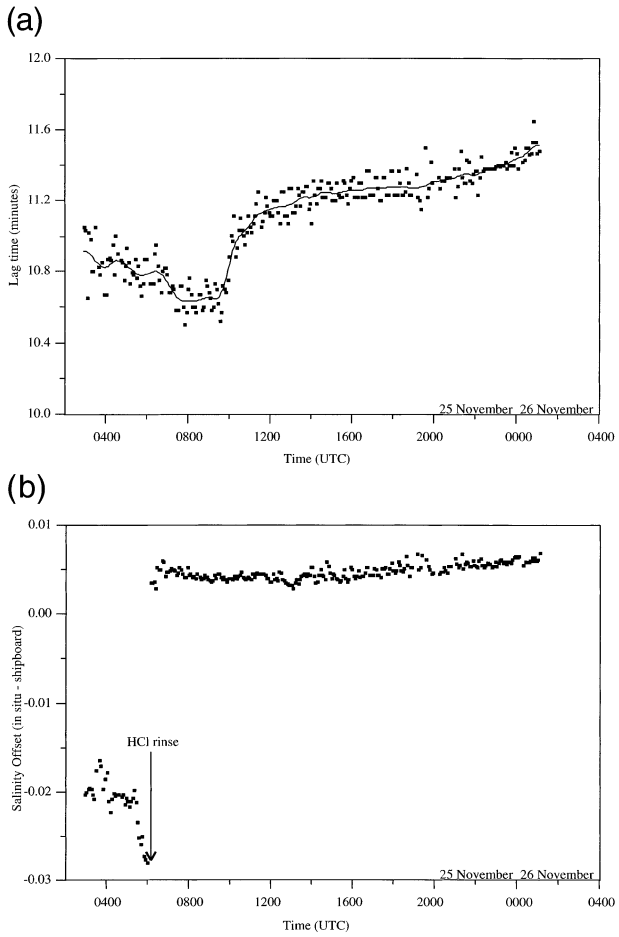

FIG. 3. (a) Time lag due to flow of sample from fish to shipboard laboratory. Individual symbols are determined by finding the combination of the time lag and sensor offset that minimizes deviation between 5-min subsets of in situ salinity data and lag-adjusted, offset-corrected shipboard data. The solid line is a 20-pass smoothing of these data. Mean absolute deviation between the 5-min lags and the smoothed fit is about 3 s. (b) Offset between salinity calculated from in situ and lag-corrected shipboard temperature and conductivity measurements (presented here as lag-adjusted shipboard salinity minus in situ salinity). The jump from a large, unstable offset of nearly -0.03 (shipboard measurements less than in situ measurements) to a fairly constant one of 0.005 corresponds to flushing of the shipboard conductivity cell with a dilute HCl solution.

5 s increases the mean absolute deviation by 50% and gives a nearly equivalent, but negative, mean deviation, demonstrating that most of the error in this case is due to offset; adjusting the lag by 10 s triples the mean absolute deviation and yields a similarly large mean deviation. Plotting the traces with suboptimal lag corrections with the in situ trace and the optimally adjusted shipboard trace emphasizes the statistical results summarized above and demonstrates the consistent mismatch between the in situ data and shipboard data adjusted with the wrong lag. Improperly adjusted shipboard data is nearly always offset from the in situ trace, without substantial overlap due to sensor noise. Finally, we compare the spatial structure of the in situ salinity field (Fig. 5a) with that reconstructed from the shipboard data (Fig. 5b). Significant error in the lag correction would have resulted in aliasing the vertical variability into the horizontal axis in Fig. 5b; however, the two fields are indistinguishable when viewed in this way.

Although the agreement between the lag-adjusted, offset-corrected shipboard salinity with that measured in situ appears to be very good, there are some real differences that we have not yet quantified. These are caused by signal smearing, or sample degradation due to mixing in the tube while transiting from the intake on the fish to the shipboard laboratory. If smearing were important on timescales approximating the residence time in the tube (at 11 min, approximately equal to the time required to move between depth minima and maxima), as had been critically suggested during early development of the system, the surface–deep variability and differences between adjacent up–down traces would be less clear in the shipboard record than in the in situ record. Figures 2–5 clearly show that this is not the case. The in situ data and the shipboard data show similar patterns and surface–deep variability. We need to examine parts of the record where sharp, short-duration features in in situ data are smoothed when they appear in the shipboard record. Such features were difficult to find in the record, but one is shown in Fig. 6, where we focus on the salinity inversion (encountered during an ascent toward the surface) seen in Fig. 4b. This feature has temporal duration of about 20 s, which corresponds to a depth range of about 5 m. The feature is noticeably smoothed in the shipboard record, with smaller amplitude and slightly broader width than seen in situ. The Reynolds number calculated for this tube and flow rate is $>10^4$; turbulent flow through a tube is known to smear input signals with a Gaussian transfer function (Fogler 1983) whose width is inversely proportional to the fluid velocity and directly proportional to the residence time in the tube. We chose to quantify this smearing by applying Gaussian filters with various time constants to the in situ data, and selecting the time constant that best approximates the shipboard trace as the one that best represents smearing in the tube. The two heavy black lines with $\tau = 7.5$ (solid) and 10 s (dashed) bracket the shipboard result fairly well, while the two light black lines with $\tau = 5$ (solid) and 15 s (dashed) significantly underestimate and overestimate, respectively, the smoothing seen in the shipboard trace. At nominal dive/climb rates of 15 m min^{-1}, this smoothing time constant corresponds to a depth interval of 1.9–2.5 m. The decrease in resolution caused by this smearing is great enough that microstructure features would be smoothed away by the time the sample reaches the ship, but is far superior to the vertical resolution attainable with traditional (e.g., Niskin bottle) sampling over similar depth intervals.

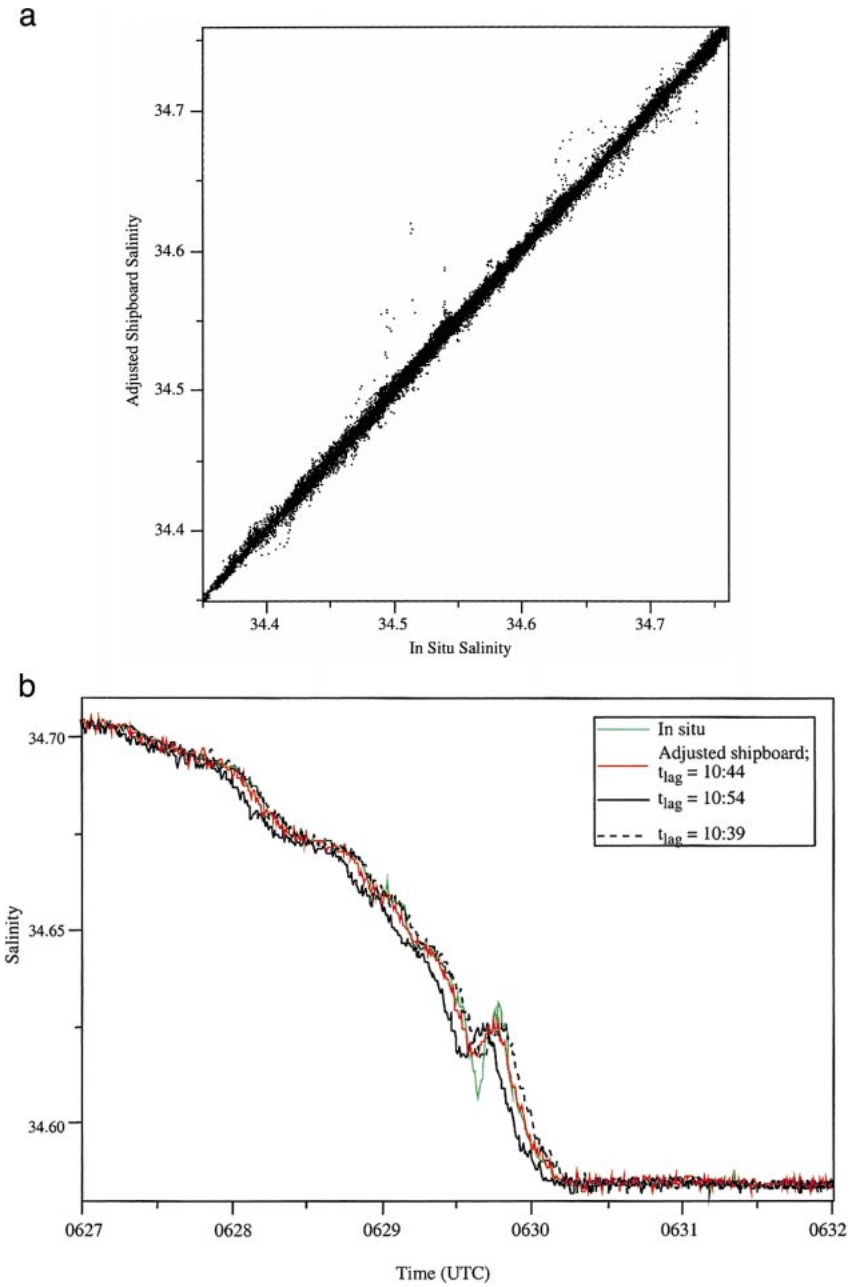

FIG. 4. (a) In situ salinity plotted vs lag- and offset-adjusted shipboard salinity. Mean absolute deviation ($N \approx 80\,000$) between the two records is 0.0015; mean deviation is <0.0001 (adjusted shipboard salinity $<10^{-4}$ greater than in situ). Most of the departures from tight correlation to the 1:1 line can be traced to instances of noise in the shipboard salinity data; others are due to smearing of sharp in situ salinity features. (b) Comparison of in situ salinity (solid green line) with adjusted shipboard salinity with various lag times for a 5-min subset of data used in determining optimum combinations of time lag and sensor offset. The adjusted shipboard salinity with the optimum lag time of 10 min, 44 s (solid red line) is a much better approximation, visually and statistically, of the in situ data than that adjusted with a lag time of 10 min, 39 s (dashed black line) or 10 min, 54 s (solid black line). Smearing of the sharp salinity inversion seen at about 0630 UTC is discussed in the text and Fig. 6.

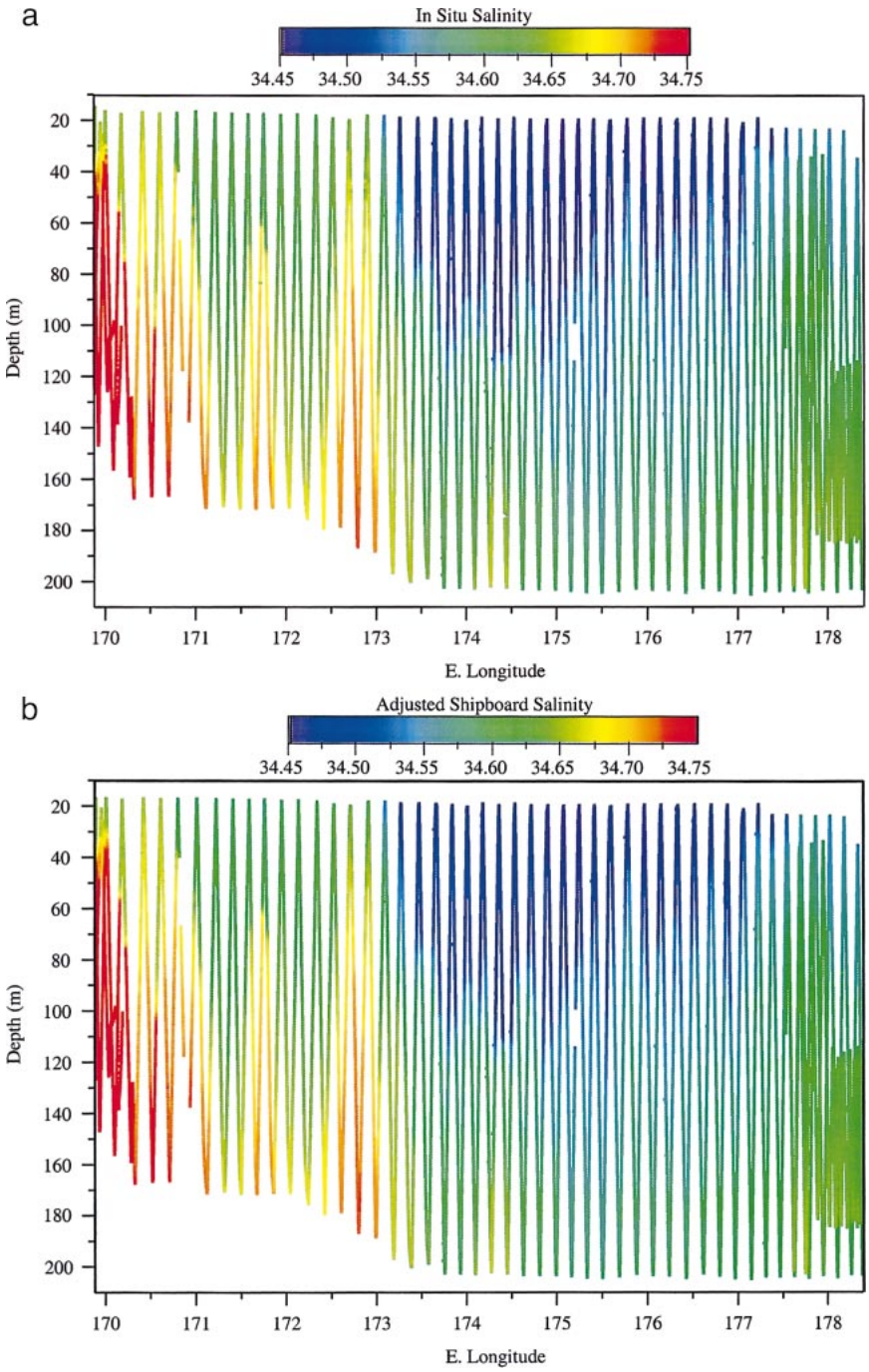

FIG. 5. Sections of salinity, indicated by the color of the symbols, as a function of depth and longitude, as determined from (a) in situ measurements and (b) lag-adjusted, offset-corrected shipboard measurements.

4. Conclusions

These results show that we can control the SeaSoar while towing with the large-diameter cable, and that we can pump seawater at ample rates from the fish to the laboratory. We can place the in situ origin of samples arriving in the laboratory with temporal resolution of a few seconds or less, regardless of the depth of the fish or its rate of change, over the ranges in these parameters experienced here. Smearing in the sample tube is well described by a center-weighted Gaussian filter with a time constant of 7.5–10 s, corresponding to about 2 m in the vertical sense at dive/climb rates of 15 m min^{-1}. We have already interfaced this sampling technology

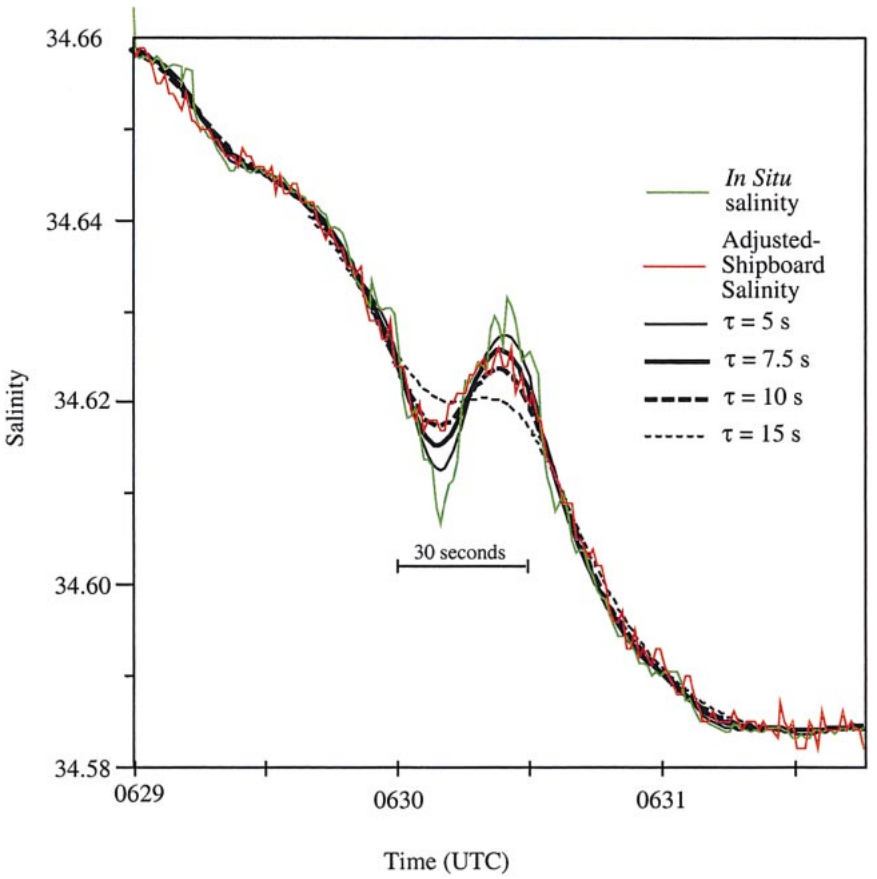

FIG. 6. In situ (solid green line) and lag-adjusted, offset-corrected shipboard (solid red line) salinity data, as in Fig. 4b, in the vicinity of a sharp in situ feature at about 0630 UTC. Other lines are in situ salinity, smoothed with Gaussian filters with the corresponding time constants. A smearing time constant of 7.5–10 applied to the in situ data seconds approximates the adjusted shipboard data well.

with high-speed measurements of the nutrient and carbon chemistry of the water pumped back to the shipboard laboratory.

Acknowledgments. We would like to thank the SeaSoar teams at the Woods Hole Oceanographic Institution and the College of Oceanic and Atmospheric Sciences at Oregon State University for their extensive, freely given advice during our development of this system. S. C. Sutherland wrote the LabView control program. B. Hales was funded during this effort by a Department of Energy Global Change Postdoctoral Fellowship.

REFERENCES

Aiken, J., 1981: The Undulating Oceanographic Recorder Mark 2. *J. Plankton Res.*, **3,** 551–560.

——, 1985: The Undulating Oceanographic Recorder Mark 2. A multirole oceanographic sampler for mapping and modeling the biophysical marine environment. *Amer. Chem. Soc.*, **209,** 315–332.

——, R. H. Bruce, and J. A. Lindley, 1977: Ecological investigations with the Undulating Oceanographic Recorder: The hydrography and plankton of the waters adjacent to the Orkney and Shetland Islands. *Mar. Biol.*, **39,** 77–91.

Bahr, F., and P. D. Fucile, 1995: SeaSoar—A flying CTD. *Oceanus*, **38,** 26–27.

Barth, J. A., and D. J. Bogucki, 2000: Spectral light absorption and attenuation measurements from a towed undulating vehicle. *Deep-Sea Res.*, **47,** 323–342.

——, ——, S. D. Pierce, and P. M. Kosro, 1998: Secondary circulation associated with a shelfbreak front. *Geophys. Res. Lett.*, **25,** 2761–2764.

——, S. D. Pierce, and R. L. Smith, 2000: A separating coastal upwelling jet at Cape Blanco, Oregon, and its connection to the California Current System. *Deep-Sea Res. II,* **47,** 783–810.

Codispoti, L. A., G. E. Friederich, J. W. Murray, and C. M. Sakamoto, 1991: Chemical variability in the Black Sea: Implications of continuous vertical profiles that penetrated the oxic/anoxic interface. *Deep-Sea Res.*, **38** (Suppl. 2), S691–S710.

Dessureault, J.-G., 1975: Batfish: A depth-controllable towed body for collecting oceanographic data. *Ocean Eng.*, **3,** 99–111.

Fogler, H. S., 1983: *Elements of Chemical Reaction Engineering.* Prentice-Hall, 769 pp.

Friederich, G. E., and L. A. Codispoti, 1987: An analysis of continuous vertical nutrient profiles taken during a cold-anomaly off Peru. *Deep-Sea Res.*, **34,** 1049–1065.

Griffiths, G., and R. T. Pollard, 1992: Tools for upper ocean surveys. *Sea Technol.*, **33,** 25–32.

Hermann, A. W., and T. M. Dauphinee, 1980: Continuous and rapid profiling of zooplankton with an electronic counter mounted on a ''Batfish'' vehicle. *Deep-Sea Res.*, **27,** 79–96.

Huyer, A., J. A. Barth, P. M. Kosro, R. K. Shearman, and R. L. Smith, 1998: Upper-ocean water mass characteristics of the California Current, summer 1993. *Deep-Sea Res. II,* **45,** 1411–1442.

Pollard, R. T., 1986: Frontal surveys with a towed profiling conductivity/temperature/depth measurement package (SeaSoar). *Nature,* **323,** 433–435.

——, J. F. Read, J. T. Allen, G. Griffiths, and A. I. Morrison, 1995: On the physical structure of a front in the Bellingshausen Sea. *Deep-Sea Res. II,* **42,** 955–982.

Press, W. H., B. P. Flannery, S. A. Teukolsky, and W. T. Vetterling, 1989: *Numerical Recipes—The Art of Scientific Computing.* Cambridge University Press.

Read, J. F., and R. T. Pollard, 1992: Water masses in the region of the Iceland–Faeroes front. *J. Phys. Oceanogr.,* **22,** 1365–1378.

Rudnick, D. L., 1996: Intensive surveys of the Azores front 2. Inferring the geostrophic and vertical velocity fields. *J. Geophys. Res.,* **101,** 16 291–16 303.

——, and J. R. Luyten, 1996: Intensive surveys of the Azores front 1. Tracers and dynamics. *J. Geophys. Res.,* **101,** 923–939.

Shearman, R. K., J. A. Barth, and P. M. Kosro, 1999: Diagnosis of the three-dimensional circulation associated with mesoscale motion in the California Current. *J. Phys. Oceanogr.,* **29,** 651–670.

Strass, V. H., 1992: Chlorophyll patchiness caused by mesoscale upwelling at fronts. *Deep-Sea Res.,* **39,** 75–96.